Published in final edited form as:
Nat Med. 2014 December ; 20(12): 1464–1471. doi:10.1038/nm.3703.

An anti-angiogenic isoform of VEGF-A contributes to impaired vascularization in peripheral artery disease

Ryosuke Kikuchi[1,2], **Kazuto Nakamura**[1], **Susan MacLauchlan**[1], **Doan Thi-Minh Ngo**[3], **Ippei Shimizu**[1], **Jose Javier Fuster**[1], **Yasufumi Katanasaka**[1], **Sumiko Yoshida**[1], **Yan Qiu**[4,8], **Terry P. Yamaguchi**[5], **Tadashi Matsushita**[6], **Toyoaki Murohara**[7], **Noyan Gokce**[3], **David O. Bates**[4,8], **Naomi M. Hamburg**[1,9], and **Kenneth Walsh**[1]

[1]Molecular Cardiology and Whitaker Cardiovascular Institute, Boston University School of Medicine, 715 Albany Street, W611, Boston, MA 02118, USA

[2]Department of Medical Technique, Nagoya University Hospital, Nagoya, Aichi 466-8550, Japan

[3]Clinical Cardiology, Department of Medicine and Whitaker Cardiovascular Institute, Boston University School of Medicine, Boston, MA 02118, USA

[4]Microvascular Research Laboratories, School of Physiology and Pharmacology, University of Bristol, Bristol BS2 8EJ, UK

[5]Cancer and Developmental Biology Laboratory, National Cancer Institute, National Institutes of Health, Frederick, MD 21701, USA

[6]Department of Clinical Laboratory, Nagoya University Hospital, Nagoya, Aichi 466-8550, Japan

[7]Department of Cardiology, Nagoya University Graduate School of Medicine, Nagoya, Aichi 466-8550, Japan

[8]Cancer Biology, Division of Cancer and Stem Cells, School of Medicine, University of Nottingham, Queen's Medical Centre, West Block, D Floor, Nottingham NG7 2UH, UK

[9]Evans Department of Medicine and the Whitaker Cardiovascular Institute, Boston University School of Medicine, 715 Albany Street, W748, Boston, MA 02118, USA

Abstract

Peripheral artery disease (PAD) generates tissue ischemia through arterial occlusions and insufficient collateral vessel formation. Vascular insufficiency in PAD occurs despite higher circulating levels of vascular endothelial growth factor A (VEGF-A),[1,2] a key regulator of angiogenesis. Here, we show that clinical PAD is associated with elevated anti-angiogenic VEGF-A splice isoform (VEGF-A_{165}b), and a corresponding reduction of the pro-angiogenic VEGF-A_{165}a isoform. In a murine model of PAD, VEGF-A_{165}b was upregulated by conditions associated with impaired limb revascularization, including leptin-deficiency, diet-induced obesity, genetic ablation of the secreted frizzled-related protein 5 (Sfrp5) adipokine and transgenic overexpression

Correspondence to: Kenneth Walsh, PhD, Molecular Cardiology/Whitaker Cardiovascular Institute, Boston University Medical Campus, 700 Albany Street, W611, Boston, MA 02118, USA, Tel.: 617-414-2390, Fax: 617-414-2391, kxwalsh@bu.edu.

of Wnt5a in myeloid cells. In PAD models, delivery of VEGF-A_{165}b inhibited revascularization of ischemic hind limbs, whereas treatment with an isoform-specific neutralizing antibody reversed the impaired revascularization phenotype caused by metabolic dysfunction or perturbations in the Wnt5a/Sfrp5 regulatory system. These results indicate that inflammation driven expression of the anti-angiogenic VEGF-A isoform can contribute to impaired collateralization in ischemic cardiovascular disease.

Keywords

VEGF-A_{165}b; VEGF-Ax; alternative splicing; translational readthrough; metabolic dysfunction

Disability attributable to PAD is rising due to an aging population and an increase in the prevalence of metabolic diseases.[3] Lower extremity ischemia in PAD is painful, disabling, causes nonhealing ulcers, and results in 200,000 amputations per year in the United States alone.[4,5] PAD thus represents a major unmet clinical need afflicting approximately 10 million people in the United States.[6] Limb ischemia induced by arterial obstructive lesions is exacerbated by insufficient angiogenesis and collateral vessel formation[7], processes regulated by VEGF-A.[8] Paradoxically, VEGF-A levels are reported to be elevated in patients with advanced PAD[2,9]. Further, clinical interventions to promote therapeutic angiogenesis by VEGF-A delivery have had limited efficacy in PAD.[10,11] It is therefore not yet clear why collateralization and angiogenesis are insufficient in patients with PAD, despite raised VEGF-A levels.

Recent work in cancer biology has identified splice variants of human VEGF-A that inhibit angiogenesis.[12,13] These isoforms arise from differential splicing of exon 8-proximal splice site usage which results in mRNA containing the initial 19 nucleotides of exon 8a, coding for pro-angiogenic VEGF-A_{165}a protein in humans, whereas distal splice site usage results in expression of exon 8b and the anti-angiogenic family of isoforms typified by VEGF-A_{165}b (Fig. 1b). VEGF-A_{165}b inhibits canonical VEGF-A signaling by competitive interference with the interaction of pro-angiogenic isoforms with the VEGFR2/NRP1 receptor complex thereby preventing full downstream signaling of VEGFR2.[13,14] However, the relevance of inhibitory VEGF-A variants to clinical ischemic syndromes including PAD remains incompletely defined and the existence of murine VEGF-A_{165}b has been questioned.[15,16] More recently, it has been reported that *VEGFA* mRNA undergoes a translational readthrough event, generating an isoform referred to as VEGF-Ax that contains a 22-amino acid extension that encompasses exons 8a and 8b, and utilizes the exon 8b stop codon.[17] Thus, there is increasing evidence to suggest that regulatory events at the 3′ portion of the *VEGFA* gene are required for the precise physiological control of VEGF-A expression.

Consistent with previous reports,[2,9] we observed higher levels of circulating VEGF-A in PAD patients compared to controls using an ELISA that does not discriminate between VEGF-A isoforms (Fig. 1a, Supplementary Table 1). To examine the relative presence of the two VEGF-A isoform families in PAD patients, serum levels were measured by western immunoblot using antibodies designed to recognize specific epitopes encoded by exon 8a or

Europe PMC Funders Author Manuscripts

8b (Fig. 1b). Total VEGF-A levels were also determined with a pan VEGF-A antibody directed against the N-terminal portion of the molecule that does not discriminate between isoforms. Consistent with the ELISA data in Fig. 1a, higher levels of total hVEGF-A were detected in the serum of PAD patients (Fig. 1b). Levels of the pro-angiogenic hVEGF-A_{165}a isoform were reduced in PAD patients relative to healthy control subjects, whereas levels of the hVEGF-A_{165}b isoform were higher in the PAD cohort (Fig. 1b). Higher expression of the inhibitory VEGF-A_{165}b isoform was associated with lower ankle-brachial index, which is used to assess the severity of PAD (Supplementary Fig. 1).

Multiple lines of evidence suggest that inflammatory cell activation contributes to the development and clinical expression of PAD.[18,19] Thus, transcript levels of h*VEGFA*$_{165}$*a* isoforms were determined in peripheral blood mononuclear cells (PBMCs) isolated from PAD patients and healthy control individuals. This analysis employed conventional RT-PCR and a primer set that amplified a region of the common *VEGFA* 3′UTR. The two VEGF-A isoforms were identified by the predicted differences in the lengths of the PCR products for *VEGFA*$_{165}$*a* and *VEGFA*$_{165}$*b* stemming from use of the proximal or distal splice sites. The shorter 60 bp fragment, predicted to generate the exon 8b-containing isoform, was preferentially represented in the PBMCs of PAD patients (Fig. 1c). In contrast, PBMCs from healthy control patients predominantly produced a 126 bp PCR fragment, consistent with use of the proximal splice site that incorporates the 8a exon. Sequence analysis of 126 bp and 60 bp PCR products confirmed the predicted exon 7/8a- and exon 7/8b exons junctions, respectively (Fig. 1c). Quantitative RT-PCR was then performed using different primer sets that specifically amplify either exon 8a- or exon 8b-containing transcripts (Fig. 1d). This analysis revealed a 61% decrease in the h*VEGFA*$_{165}$*a* transcript and a 4.6-fold increase in the h*VEGFA*$_{165}$*b* transcript in the PBMC of PAD patients relative to healthy control individuals. Higher PBMC expression of *VEGFA*$_{165}$*b* transcript was strongly associated with higher serum levels of VEGF-A_{165}b ($r=0.65$, $P < 0.0001$; data not shown).

Emerging evidence has linked non-canonical Wnt5a signaling to the control of vascularization in mouse retina through changes in the splice pattern of *VEGFR1*, giving rise to soluble fms-like tyrosine kinase-1 (sFlt-1) that functions as a negative regulator of angiogenesis.[20,21] To evaluate the potential involvement of noncanonical WNT signaling in VEGF-A splicing, *WNT5A* levels were assessed in PBMCs from healthy control and PAD patients. Higher levels of *WNT5A* gene expression were detected in PBMCs from patients with PAD (Supplementary Fig. 2a). In contrast, we found similar levels of *sFLT1* expression in PBMCs from PAD patients compared to controls (Supplementary Fig. 2b). To evaluate the cell population accountable for the increased *WNT5A* gene expression in PBMCs in PAD patients, two major cellular fractions (monocytes and non-monocytes) were separated from the PBMC samples for a subset of patients and healthy controls. In both groups, *WNT5A* gene expression was significantly higher in the monocyte vs. the non-monocyte fraction, suggesting that *WNT5A* is highly expressed in cells of the monocyte/macrophage lineage (Supplementary Fig. 2c). In addition, *WNT5A* transcript levels in circulating monocytes were significantly upregulated in PAD patients compared with healthy controls, similar to observations in whole PBMCs samples. Consistent with the concept that *WNT5A* signaling regulates VEGF-A isoform levels, *WNT5A* expression in PBMC was positively associated

with serum levels of VEGF-A_{165}b (Supplementary Fig. 3a), and there was a negative association between *WNT5A* expression in PBMC and ankle-brachial index (Supplementary Fig. 3b).

To investigate whether Wnt5a is functionally relevant to the control of *Vegfa* alternative splicing in ischemia-induced regenerative angiogenesis, we employed a murine model of PAD. PAD is simulated by unilateral resection of the femoral artery which leads to a hemodynamic deficit that can be monitored non-invasively by laser Doppler blood flow imaging (LDBF) and anatomically by measuring capillary density. We observed a relatively modest upregulation of Wnt5a in the ischemic limbs of wild-type C57BL/6, both at the level of protein and mRNA (Supplementary Fig. 4a,b). Immunohistochemical analyses of the ischemic limbs revealed Wnt5a colocalization with Mac2-positive cells, indicating that macrophages are a source of Wnt5a in this model (Supplementary Fig. 4c).

To examine the involvement of Wnt5a in the regulation of *Vegfa* splicing, mice overexpressing Wnt5a in myeloid cells were constructed by crossing Lysozyme M-Cre (LysM-Cre) mice with knock-in mice carrying a Cre-inducible Wnt5a transgene (Supplementary Fig. 5a). Compared with wild-type mice, LysM-$Wnt5a^{GOF}$ mice expressed higher levels of Wnt5a protein and mRNA in hind limbs following ischemic surgery (Supplementary Fig. 5b,c) and this was associated with the increased expression of the macrophage marker protein Mac2 (Supplementary Fig. 5d). Although LysM-$Wnt5a^{GOF}$ mice display no detectable baseline phenotype, they had impaired revascularization as determined by LDBF imaging in response to surgical ischemia (Fig. 2a). Correspondingly, the gastrocnemius muscle of the Wnt5a transgenic mice displayed an inability to increase capillary density in response to ischemia as assessed in histological sections stained with anti-CD31 antibody (Fig. 2b) or isolectin IB4 (data not shown). Consistent with the findings in human PAD, serum levels of total murine VEGF-A were elevated in LysM-$Wnt5a^{GOF}$ mice at 7 days post-surgery, using an ELISA that does not discriminate between isoforms (Fig. 2c). Using a pan-VEGF-A antibody, Western blot analysis of gastrocnemius muscle also revealed an increase in tissue levels of total VEGF-A in response to ischemia, which was further amplified in the Wnt5a transgenic mice (Fig. 2d). Employing an antibody that specifically recognizes the previously reported sequence encoded by c-terminal exon, hereafter referred to as murine exon 8a, an upregulation of VEGF-A_{164}a could be detected in the ischemic limbs of wild-type mice, but not LysM-$Wnt5a^{GOF}$ mice. These assays revealed a striking discrepancy between the levels of total VEGF-A and the exon 8a-containing isoform in the ischemic limbs of the transgenic mice. Moreover, despite an overall increase in total VEGF-A expression in the ischemic limbs of LysM-$Wnt5a^{GOF}$ mice, tyrosine phosphorylation of VEGFR2 was not activated, indicative of impaired VEGF-A signaling under these conditions (Supplementary Fig. 6).

Because the structure of the putative murine VEGF-A_{165}b has not been described previously, PCR primers that span the c-terminal exons and the 3′-UTR region of the *Vegfa* transcript were constructed (Supplementary Fig. 7). Conventional PCR analysis of mRNA isolated from the ischemic gastrocnemius muscle of wild-type mice revealed a PCR product fragment of 281 bp that is expected from the pro-angiogenic *$Vegfa_{164}a$* transcript (Fig. 2e). Sequence analysis of this fragment confirmed the exon 7/8a splice event that is predicted to

encode the previously reported 6 amino acid terminal portion of murine VEGF-A_{164}a (Fig. 2f).[22] In contrast, RT-PCR analysis of limbs from the LysM-Wnt5a^{GOF} mice detected a reduction in the 281 bp fragment of *Vegfa$_{164}$a* and the appearance of a new band at 215 bp (Fig. 2e). Sequence analysis of this product revealed that this transcript is derived from use of the distal splice junction where exon 7 is joined to a new exon, hereafter referred to as murine exon 8b (Fig. 2f). Murine exon 8b contains a 7 amino acid open reading frame followed by a stop codon, that is predicted to contribute to the translation of a full-length, mature protein that is 165 amino acids in length and highly homologous to human VEGF-A_{165}b (Supplementary Fig. 8), and is hereafter referred to as mVEGF-A_{165}b.

Since mouse VEGF-A_{165}b has not been characterized, qPCR primers specific for the junction of 7/8a (m*Vegfa$_{164}$a* primers) or 7/8b (m*Vegfa$_{165}$b* primers) were designed and validated (Supplementary Fig. 9). Quantitative RT-PCR analysis of these isoforms in murine hind limb revealed that the ischemia surgery led to a 70% increase in the *Vegfa$_{164}$a* isoform in wild-type mice, but levels of this transcript declined by a factor of 3 in mice overexpressing Wnt5a in myeloid cells (Supplementary Fig. 10). In contrast, there was a marked elevation in *Vegfa$_{165}$b* isoform expression in the ischemic hind limbs of the transgenic strain. To analyze the regulation of the protein encoded by the murine *Vegfa$_{165}$b* transcript, an antibody was produced to the predicted exon 8b hexapeptide. This antibody did not cross react with the VEGF-A_{164}a protein in immunoblot analyses, and the exon 8b-encoded epitope could be detected in the total VEGF-A immunoprecipitated from the ischemic limbs of the transgenic mice (Supplementary Fig. 11). Using this antibody, the upregulation of the exon 8b-containing isoform, i.e. VEGF-A_{165}b, could be detected in the ischemic hind limb of the LysM-Wnt5a^{GOF} mice (Fig. 2g).

Western immunoblot analysis was also performed using an antibody that recognizes the *VEGFA* translational readthrough product that is referred to as VEGF-Ax (Supplementary Fig. 12a). In contrast to findings with the antibody that recognizes the exon 8b hexapeptide, that is predicted to be present in both VEGF-A_{165}b and VEGF-Ax isoforms, no immunoreactive material could be detected in the ischemic limbs of Wnt5a or wild-type mice when immunoblots were probed with the antibody that recognizes the highly conserved Ax peptide that is uniquely present in the readthrough product of VEGF-Ax (Supplementary Fig. 12b). Because VEGF-Ax is reported to be widely expressed in human tissues,[17] a subset of serum samples from PAD patients and healthy control subjects was reanalyzed using antibodies that specifically recognize the unique readthrough portion of VEGF-Ax or the terminal hexapeptide that is encoded by exon 8b. This analysis detected Ax peptide-immunoreactive material in both healthy control and PAD patient sera, but, unlike the immunoblot with the exon 8b-specific antibody, no difference was detected in the levels of the Ax epitope (Supplementary Fig. 12c).

To explore the functional significance of mVEGF-A_{165}b, an adenoviral vector expressing this isoform was constructed and administered to wild-type mice prior to ischemic hind limb surgery. Flow recovery in Ad-m*Vegfa$_{165}$b* -treated mice was significantly less than control by the third day after surgery, and the flow difference persisted throughout the time course of the experiment (Fig. 2h). Quantitative analysis of CD31-positive cells in gastrocnemius muscle on post-operative day 14 revealed that the ischemia-induced increase in capillary

density was not observed in the Ad-m*Vegfa*$_{165}$*b*-treated mice compared with control mice (Fig. 2h), corroborating the LDBF data. Because mVEGF-A$_{165}$b is upregulated in LysM-Wnt5a^{GOF} mice, these animals were treated with an exon 8b-specific neutralizing antibody (Supplementary Fig. 13), and then subjected to hind limb ischemic surgery to assess the function of the endogenous isoform. Mice receiving VEGF-A$_{165}$b neutralizing antibody displayed improved blood flow reperfusion and increased capillary density in the affected limb compared with LysM-Wnt5a^{GOF} mice receiving an equivalent dose of IgG control antibody (Fig. 2i). In contrast, wild-type mice that did not display an appreciable increase in mVEGF-A$_{165}$b expression following ischemic surgery are refractory to treatment with the neutralizing antibody. Collectively, these results show that macrophage expression of Wnt5a inhibits regenerative angiogenesis, at least in part, through the upregulation of mVEGF-A$_{165}$b.

Sfrp5 is predominantly expressed by adipose tissue where it inhibits inflammation by suppressing non-canonical Wnt5a signaling in macrophages.[23] Therefore, the effect of Sfrp5-deficiency on ischemia-induced angiogenesis and VEGF-A$_{165}$b expression was evaluated. As with the LysM-Wnt5a^{GOF} mice, Sfrp5-deficiency also led to impaired reperfusion and capillarity of ischemic limbs in the PAD model (Supplementary Fig. 14a,b). To assess the molecular basis for the angiogenic deficiency in the Sfrp5-KO mice, qRT-PCR was performed to analyze the expression patterns of *Wnt* family members in the gastrocnemius muscle of the different experimental groups of mice. Of the 19 *Wnt* family members, only *Wnt5a* transcript displayed a significant increase in expression in the ischemic limbs of Sfrp5-KO mice (Supplementary Fig. 14c). Western immunoblot assays were then performed to assess Wnt-5a protein levels under these experimental conditions. As with the transcript levels, Wnt-5a protein expression was markedly upregulated in the ischemic limb muscle of Sfrp5-KO mice (Supplementary Fig. 14d), attributable to a greater influx of Mac2/Wnt-5a double-positive macrophages under these conditions (Supplementary Fig. 14e). Consistent with these findings, immunoblot analysis revealed that Sfrp5-deficiency led to a marked increase in Mac2 expression in the ischemic limb but had no effect on Mac2 expression in the uninjured contralateral limb (Supplementary Fig. 14f). Thus, Sfrp5-deficiency phenocopies the LysM-Wnt5a^{GOF} transgenic mouse model with regard to regenerative angiogenesis and macrophage infiltration in ischemic limbs, and this model represents an additional system to address the role of mVEGF-A$_{165}$b isoform. Hind limb muscle from these experimental groups of Sfrp5-KO mice were probed for total murine VEGF-A, VEGF-A$_{164}$a and VEGF-A$_{165}$b expression by immunoblotting. As with the LysM-Wnt5a^{GOF} model, Sfrp5-deficiency was associated with an increase in total VEGF-A protein expression, both in the ischemic tissue and in the serum, but this was not accompanied by an increase in the mVEGF-A$_{164}$a isoform that encodes exon 8a (Supplementary Fig. 14g,h). Instead, Sfrp5-deficiency led to an increase in mVEGF-A$_{165}$b. Isoform-specific qPCR of transcripts in the ischemic and non-ischemic gastrocnemius muscle revealed a modest upregulation of the exon 8a-containing m*Vegfa*$_{164}$*a* isoform in wild-type mice post-surgery. However, the exon 8b-containing m*Vegfa*$_{165}$*b* isoform was selectively upregulated in the ischemic muscle of the Sfrp5-KO mice (Supplementary Fig. 14i). To assess the functional significance of mVEGF-A$_{165}$b upregulation under these experimental conditions, Sfrp5-KO mice were administered the anti-VEGF-A$_{165}$b

neutralizing antibody or control IgG prior to hind limb surgery. Ischemic limbs of mice receiving the neutralizing antibody had increased reperfusion as determined by LDBF (Supplementary Fig. 14j). Consistent with these data, Sfrp5-KO mice treated with the neutralizing antibody displayed an increase in capillary density in the gastrocnemius muscle of the ischemic limb relative to the contralateral control limb, whereas Sfrp5-KO mice treated with IgG showed no increase in capillary density in muscle following ischemic surgery. Collectively, these data reveal that both Sfrp5-KO and LysM-Wnt5a^{GOF} mice upregulate the anti-angiogenic mVEGF-A$_{165}$b splice variant in response to ischemia, and this contributes to impaired angiogenic responses in these models.

PAD is strongly associated with diabetes mellitus,[24] and studies in experimental models have shown that metabolic dysfunction leads to a reduction in the angiogenic response to tissue ischemia.[25] Because perturbations in the Sfrp5-Wnt5a regulatory system contribute to systemic metabolic dysfunction under conditions of obesity,[23] we evaluated the regulation and function of the anti-angiogenic mVEGF-A$_{165}$b in models of diet-induced obesity and leptin-deficiency. Consistent with observations in adipose tissue,[23] Wnt5a protein and mRNA expression were elevated in the ischemic muscle of mice fed a high fat/high sucrose (HF/HS) diet or ob/ob mice relative to mice fed a standard chow diet or C57Bl/6J mice, respectively (Fig. 3a,b, Supplementary Fig. 15a,b). The increase in Wnt5a in muscle tissue under conditions of metabolic dysfunction resulted from an increase in the infiltration of Wnt-5a/Mac2 double-positive macrophages (Fig. 3c, Supplementary Fig. 15c). Western blot analysis of gastrocnemius muscle from these experimental groups of mice revealed the upregulation of VEGF-A expression, in both the HF/HS-fed and ob/ob mice, using a pan-VEGF-A antibody that does not discriminate between the isoforms (Fig. 3d, Supplementary Fig. 15d). Isoform-specific antibodies revealed modest upregulation of the mVEGF-A$_{164}$a isoform in ischemic limbs of metabolically normal mice, but the HF/HS-fed and ob/ob mice displayed marked elevations in the anti-angiogenic mVEGF-A$_{165}$b isoform. Lysates from the ischemic limbs of ob/ob mice (Supplementary Fig. 15e) and HF/HS-fed mice (data not shown) were probed with antibodies specific for the unique VEGF-Ax extension peptide versus the exon 8b-encoded hexapeptide. Whereas the exon 8b material could be detected in ob/ob mice, no Ax extension peptide-containing material could be detected under the conditions of our assays. Corroborating the findings with the isoform-specific antibodies, isoform specific qPCR of *Vegfa* cDNA isolated from gastrocnemius muscle revealed that metabolic dysfunction led to a reduction in the expression of the pro-angiogenic *Vegfa* isoform and an increase in anti-angiogenic exon 8b-containing isoform (Fig. 3e, Supplementary Fig. 15f). HF/HS-fed and ob/ob mice both display impaired revascularization as assessed by LDBF imaging, capillary and arteriole density analyses (Fig. 3f, Supplementary Figs. 15g and 16). To assess the functional significance of mVEGF-A$_{165}$b under these conditions of metabolic dysfunction, both ob/ob and HF/HS-fed C57Bl/6 mice were treated with anti-VEGF-A$_{165}$b neutralizing antibody or IgG control and subjected to hind limb ischemic surgery. Whereas the neutralizing antibody had no effect on the angiogenic response in metabolically normal mice, both the HF/HS-fed and ob/ob mice treated with this reagent showed significant improvements in the revascularization of their ischemic limbs (Fig. 3f, Supplementary Figs. 15g and 16).

To examine the regulation of VEGF-A_{165}b at a mechanistic level, cultured RAW264.7 cells, a mouse macrophage line, were treated with recombinant Wnt5a. Wnt5a-stimulation led to a dose-dependent increase in VEGF-A_{165}b (Fig. 4a), and the upregulation of this *Vegfa* splice variant could also be detected at the level of mRNA (Fig. 4b). Consistent with the finding that Wnt5a signals in a non-canonical manner,[26] knockdown of Ror2, a Frizzled co-receptor protein, abolished Wnt5a-mediated *$Vegfa_{165}b$* induction (Fig. 4b). Also consistent with a non-canonical signaling mechanism, Wnt5a treatment led to the activation of JNK (Fig. 4c), and pretreatment with the JNK inhibitor SP600125 abolished Wnt5a-mediated *$Vegfa_{165}b$* expression (Fig. 4d). Similarly, treatment with recombinant Sfrp5 protein blocked VEGF-A_{165}b expression under these conditions. Further investigation revealed that Wnt5a upregulated the expression of SC35, a pre-mRNA splicing factor implicated in the alternative processing of *Vegfa* at exon 8,[27] in a JNK- and Sfrp5-dependent manner (Fig. 4e). Knockdown of SC35 blocked the Wnt5a-mediated induction of *$Vegfa_{165}b$* (Fig. 4f). Collectively, these data suggest that Wnt5a promotes the processing of *Vegfa* to the exon 8b-containing isoform, at least in part, via an Ror2/JNK/SC35-dependent mechanism (Fig. 4g).

Here, we show that the anti-angiogenic splice variant of VEGF-A is expressed in clinical and experimental settings that are associated with impaired vascularization. It has been noted previously, and confirmed here, that total VEGF-A levels are paradoxically elevated in patients with PAD.[2,9] Using isoform-specific antibodies, we provide evidence that the circulating VEGF-A in PAD patients is predominantly comprised of the variant VEGF-A_{165}b isoform. In murine experimental models we establish the presence mVEGF-A_{165}b and define its regulation by conditions that contribute to systemic metabolic dysfunction. In contrast, we did not detect the VEGF-Ax isoform in the ischemic limbs of these murine models. While VEGF-Ax appeared to be present in human serum, its upregulation was not observed in a small cohort of PAD patients. However, VEGF-Ax regulation should be further evaluated using larger sample sizes as well as different clinical cohorts. We also demonstrate, for the first time, that the VEGF-A_{165}b isoform impairs revascularization in a model of PAD. Conversely, acute immunological neutralization of mVEGF-A_{165}b promotes revascularization of ischemic tissue under conditions where the process of regenerative angiogenesis is impaired. These findings support the concept that VEGF-A_{165}b may represent a new pharmacological target to treat limb ischemia in patients with PAD, and that its neutralization may augment the activities of pro-angiogenic growth factors.

Metabolic diseases, including diabetes and obesity, promote ischemic cardiovascular diseases, but the molecular mechanism underlying this pathological process remain incompletely defined. Obesity-linked changes in the expression of adipose tissue-derived Sfrp5 can lead to overactivation of non-canonical Wnt5a signaling in macrophages that, in turn, promotes inflammation and systemic metabolic dysfunction, but the link between this signaling and vascular disease was not known.[23] We now show that Sfrp5 deficiency impairs hind limb revascularization response to ischemia. This impairment is associated with greater infiltration of activated, Wnt5a-positive macrophages in the ischemic tissue. Myeloid-specific Wnt5a overexpression of Wnt5a parallels Sfrp5 deficiency with exaggerated macrophage infiltration and blunted revascularization in ischemic limbs. In both models, we demonstrated upregulation of the mVEGF-A_{165}b isoform in ischemic tissue and

Europe PMC Funders Author Manuscripts

that immunological neutralization of the inhibitory VEGF-A isoform promotes the angiogenic response to ischemia. These data indicate that Wnt5a, and its upstream effector Sfrp5, mediate the effects of metabolic dysfunction on regenerative angiogenesis by controlling macrophage expression of VEGF-A_{165}b. Taken together, our findings identify the Sfrp5-Wnt5a-VEGF-A_{165}b axis as a novel regulator of the vascular response to ischemia in the setting of metabolic diseases, and provide a novel potential mechanism for the link between obesity and cardiovascular disease.

Supplementary Material

Refer to Web version on PubMed Central for supplementary material.

Acknowledgements

This work was supported by National Institutes of Health grants HL102874, AG34972, and HL68758 to K. Walsh. R. Kikuchi is supported by the Uehara Memorial Foundation and Grant-in-Aid for Young Scientists B. N. Hamburg is supported by National Institutes of Health grants HL102299 and HL109790, and N. Gokce is supported by National Institutes of Health grants HL081587 and HL1145675. D. Bates is supported by the British Heart Foundation, Wellcome Trust, Cancer Research UK and the MRC. We are grateful to Drs. Sandeepa M. Eswarappa and Paul L. Fox for providing anti-Ax specific antibody and recombinant VEGF-Ax protein.

References

1. Blann AD, et al. Vascular endothelial growth factor and its receptor, Flt-1, in the plasma of patients with coronary or peripheral atherosclerosis, or Type II diabetes. Clin. Sci. (Lond.). 2002; 102:187–194.
2. Findley CM, Mitchell RG, Duscha BD, Annex BH, Kontos CD. Plasma levels of soluble Tie2 and vascular endothelial growth factor distinguish critical limb ischemia from intermittent claudication in patients with peripheral arterial disease. J. Am. Coll. Cardiol. 2008; 52:387–393. [PubMed: 18652948]
3. Murray CJ, et al. Disability-adjusted life years (DALYs) for 291 diseases and injuries in 21 regions, 1990-2010: a systematic analysis for the Global Burden of Disease Study 2010. Lancet. 2013; 380:2197–2223. [PubMed: 23245608]
4. Hamburg NM, Balady GJ. Exercise rehabilitation in peripheral artery disease: functional impact and mechanisms of benefits. Circulation. 2011; 123:87–97. [PubMed: 21200015]
5. Anderson PL, et al. Understanding trends in inpatient surgical volume: vascular interventions, 1980-2000. J. Vasc. Surg. 2004; 39:1200–1208.
6. Go AS, et al. Heart disease and stroke statistics--2013 update: a report from the American Heart Association. Circulation. 2013; 127:e6–e245. [PubMed: 23239837]
7. Duscha BD, et al. Angiogenesis in skeletal muscle precede improvements in peak oxygen uptake in peripheral artery disease patients. Arterioscler. Thromb. Vasc. Biol. 2011; 31:2742–2748.
8. Carmeliet P, Jain RK. Molecular mechanisms and clinical applications of angiogenesis. Nature. 2011; 473:298–307. [PubMed: 21593862]
9. Makin AJ, Chung NA, Silverman SH, Lip GY. Vascular endothelial growth factor and tissue factor in patients with established peripheral artery disease: a link between angiogenesis and thrombogenesis? Clin. Sci. (Lond.). 2003; 104:397–404. [PubMed: 12653684]
10. Makinen K, et al. Increased vascularity detected by digital subtraction angiography after VEGF gene transfer to human lower limb artery: a randomized, placebo-controlled, double-blinded phase II study. Mol. Ther. 2002; 6:127–133.
11. Rajagopalan S, et al. Regional angiogenesis with vascular endothelial growth factor in peripheral arterial disease: a phase II randomized, double-blind, controlled study of adenoviral delivery of vascular endothelial growth factor 121 in patients with disabling intermittent claudication. Circulation. 2003; 108:1933–1938. [PubMed: 14504183]

12. Bates DO, et al. Association between VEGF splice isoforms and progression-free survival in metastatic colorectal cancer patients treated with bevacizumab. Clin. Cancer Res. 2012; 18:6384–6391. [PubMed: 23104894]
13. Kawamura H, Li X, Harper SJ, Bates DO, Claesson-Welsh L. Vascular endothelial growth factor (VEGF)-A165b is a weak in vitro agonist for VEGF receptor-2 due to lack of coreceptor binding and deficient regulation of kinase activity. Cancer Res. 2008; 68:4683–4692. [PubMed: 18559514]
14. Cebe Suarez S, et al. A VEGF-A splice variant defective for heparan sulfate and neuropilin-1 binding shows attenuated signaling through VEGFR-2. Cell. Mol. Life Sci. 2006; 63:2067–2077. [PubMed: 16909199]
15. Jones WS, et al. Alteration in angiogenic and anti-angiogenic forms of vascular endothelial growth factor-A in skeletal muscle of patients with intermittent claudication following exercise training. Vasc. Med. 2012; 17:94–100. [PubMed: 22402934]
16. Dokun AO, Annex BH. The VEGF165b “ICE-o-form” puts a chill on the VEGF story. Circ. Res. 2011; 109:246–247. [PubMed: 21778432]
17. Eswarappa SM, et al. Programmed translational readthrough generates antiangiogenic VEGF-Ax. Cell. 2014; 157:1605–1618. [PubMed: 24949972]
18. McDermott MM, et al. Elevated levels of inflammation, d-dimer, and homocysteine are associated with adverse calf muscle characteristics and reduced calf strength in peripheral arterial disease. J. Am. Coll. Cardiol. 2007; 50:897–905. [PubMed: 17719478]
19. Vidula H, et al. Biomarkers of inflammation and thrombosis as predictors of near-term mortality in patients with peripheral arterial disease: a cohort study. Ann. Intern. Med. 2008; 148:85–93. [PubMed: 18195333]
20. Stefater JA 3rd, et al. Regulation of angiogenesis by a non-canonical Wnt-Flt1 pathway in myeloid cells. Nature. 2011; 474:511–515. [PubMed: 21623369]
21. Kendall RL, Thomas KA. Inhibition of vascular endothelial cell growth factor activity by an endogenously encoded soluble receptor. Proc. Natl. Acad. Sci. U. S. A. 1993; 90:10705–10709. [PubMed: 8248162]
22. Tischer E, et al. The human gene for vascular endothelial growth factor. Multiple protein forms are encoded through alternative exon splicing. J. Biol. Chem. 1991; 266:11947–11954. [PubMed: 1711045]
23. Ouchi N, et al. Sfrp5 is an anti-inflammatory adipokine that modulates metabolic dysfunction in obesity. Science. 2010; 329:454–457. [PubMed: 20558665]
24. Marso SP, Hiatt WR. Peripheral arterial disease in patients with diabetes. J. Am. Coll. Cardiol. 2006; 47:921–929. [PubMed: 16516072]
25. Schiekofer S, Galasso G, Sato K, Kraus BJ, Walsh K. Impaired revascularization in a mouse model of type 2 diabetes is associated with dysregulation of a complex angiogenic-regulatory network. Arterioscler. Thromb. Vasc. Biol. 2005; 25:1603–1609. [PubMed: 15920034]
26. Ho HY, et al. Wnt5a-Ror-Dishevelled signaling constitutes a core developmental pathway that controls tissue morphogenesis. Proc Natl Acad Sci U S A. 2012; 109:4044–4051. [PubMed: 22343533]
27. Merdzhanova G, et al. The transcription factor E2F1 and the SR protein SC35 control the ratio of pro-angiogenic versus antiangiogenic isoforms of vascular endothelial growth factor-A to inhibit neovascularization in vivo. Oncogene. 2010; 29:5392–5403. [PubMed: 20639906]

Europe PMC Funders Author Manuscripts

Europe PMC Funders Author Manuscripts

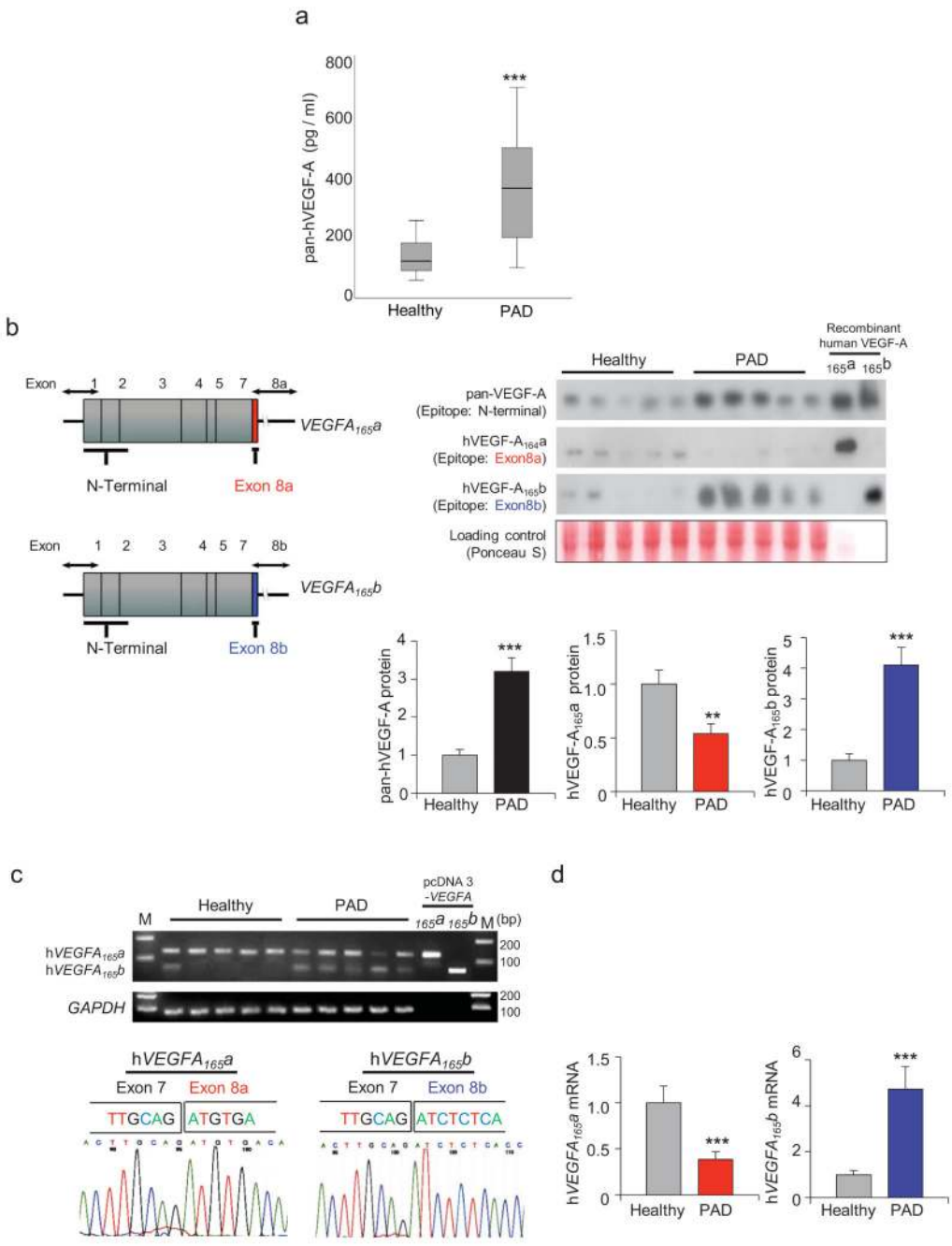

Figure 1. Circulating levels of total VEGF-A, VEGF-A$_{165}$a and VEGF-A$_{165}$b in PAD patients

a, Total VEGF-A was measured by ELISA in the serum of PAD (n = 18) and healthy (n = 17) subjects using an antibody that does not discriminate between isoforms. Data are presented as box plots indicating median, upper and lower quartiles. **b**, A schematic of the exon structure of *VEGFA$_{165}$a* (top) and *VEGFA$_{165}$b* (bottom) demonstrating the regions recognized by the N-terminal "pan" VEGF-A exon 8a and exon 8b antibodies. Serum protein expression of total hVEGF-A, hVEGF-A$_{165}$a and hVEGF-A$_{165}$b were measured in PAD (n = 18) and healthy (n = 19) subjects by western blot analysis. Relative pan-hVEGF-

A, hVEGF-A_{165}a and hVEGF-A_{165}b were quantified using ImageJ. Immunoblots were normalized to loading control signal. Results are shown as the mean ± S.E. **c**, Conventional PCR of mRNA extracted from PBMCs of PAD and healthy subjects using primers that detect both proximal, h*VEGFA*$_{165}$*a* (126 bp), and distal splice, h*VEGFA*$_{165}$*b* (60 bp), splicing events of exon 8 in human VEGF-A. pcDNA3-*VEGFA*$_{165}$*a* and *VEGFA*$_{165}$*b* plasmid were used as a positive controls. Sequencing of the 126bp product (bottom left panel) and 60 bp product (bottom right panel) from 5 PAD patients and 5 healthy control individuals, respectively, reveal the bands arise from the expected splicing events. d, h*VEGFA*$_{165}$*a* and h*VEGFA*$_{165}$*b* mRNA expression was measured by qRT-PCR using peripheral blood mononuclear cells from PAD (n = 25) and healthy (n = 25) subjects. All analyses by Independent Samples Kolmogorov-Smirnov Test. $^{**}P < 0.01$, $^{***}P < 0.001$.

Europe PMC Funders Author Manuscripts

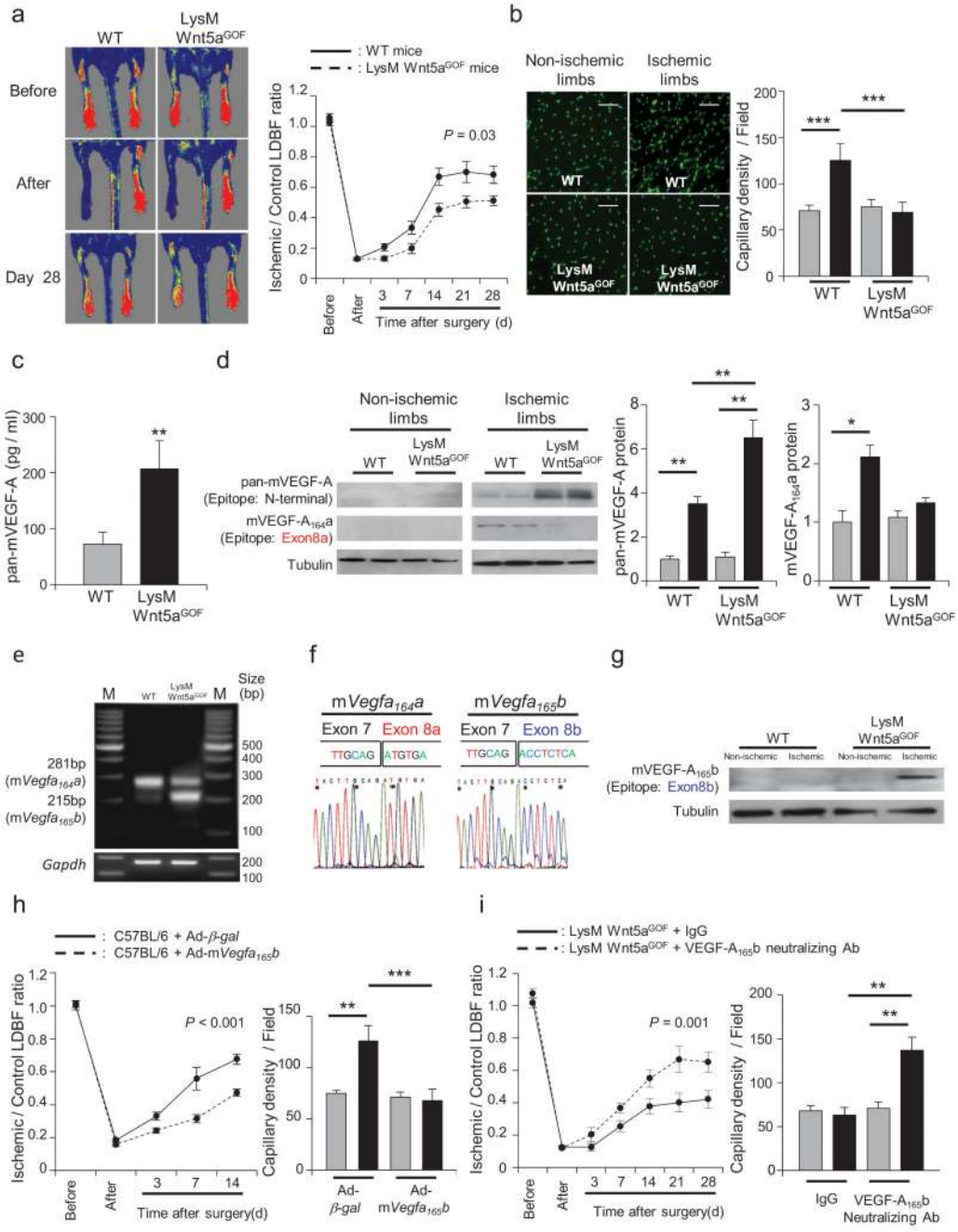

Figure 2. Myeloid specific Wnt5a impairs ischemia-induced angiogenesis in mice by a mechanism requiring VEGF-A$_{165}$b

a, Representative LDBF images in the ischemic limbs of Wild-type or LysM-Wnt5a^{GOF} mice. Quantitative analysis of the ischemic/non-ischemic (control) LDBF ratio in wild-type (WT) or LysM-Wnt5a^{GOF} mice by postoperative day 28. Results are shown as the mean ± S.E. (n = 12) Repeated measures ANOVA. **b**, Immunostaining of gastrocnemius in contralateral non-ischemic (gray bar) and ischemic (black bar) tissues with anti-CD31 monoclonal antibody (green in tissue sections). Quantitative analysis of capillary density in WT or LysM-Wnt5a^{GOF} mice was performed on postoperative day 28. Capillary density

Europe PMC Funders Author Manuscripts

was expressed as the number of capillaries per high power field (×200). Scale bars are 100 μm. Results are shown as the mean ± S.E. (n = 5/group). ANOVA with post-hoc Tukey HSD. **c**, Circulating levels of total mVEGF-A was measured in WT and LysM-Wnt5a^{GOF} mice by ELISA employing a pan-VEGF-A antibody at 7 days after surgery. Results are shown as the mean ± S.E. (n = 8/group) Independent samples t-test. **d**, Total mVEGF-A and mVEGF-A$_{164}$a isoform protein expression were determined by western blot analysis in contralateral non-ischemic (gray bar) and ischemic (black bar) muscle at 7 days after surgery. A representative blot from three independent experiments is shown. Relative levels of total mVEGF-A and mVEGF-A$_{164}$a protein were quantified using ImageJ. Immunoblots were normalized to the tubulin signal. Results are shown as the mean ± S.E. (n = 5/group). ANOVA with post-hoc Tukey HSD. **e**, Conventional PCR of mRNA from WT and LysM-Wnt5a^{GOF} gastrocnemius muscle 7 days after hind limb ischemia surgery using primers that span both the proximal and distal splice sites (m*Vegfa*$_{164}$*a* and m*Vegfa*$_{165}$*b*). **f**, Sequence results of the 281bp (left panel) and 215bp (right panel) PCR products from the agarose gel in Fig. 2f indicating the splice junctions of m*Vegfa*$_{164}$*a* and m*Vegfa*$_{165}$*b*. **g**, Using an antibody that recognizes the peptide encoded by murine exon 8b, mVEGF-A$_{165}$b protein expression was determined by western blot analysis in contralateral non-ischemic (gray bar) and ischemic (black bar) muscle at 7 days after surgery. A representative blot from three independent experiments is shown. **h**, Ad-m*Vegfa*$_{165}$*b* or Ad-*β-gal* (control) was injected into the jugular vein of WT mice (2×10^9 pfu in each group) at 3 days prior to ischemic hind limb surgery. Analysis of the ischemic/non-ischemic laser Doppler blood flow ratio in Ad-m*Vegfa*$_{165}$*b*-treated and control WT mice through postoperative day 14 is shown. Results are shown as the mean ± S.E. (n = 10/group). Repeated measures ANOVA. Quantitative analysis of capillary density by anti-CD31 antibody in Ad-m*Vegfa*$_{165}$*b*-treated or control mice on postoperative day 14. Capillary density was expressed as the number of capillaries per high power field (×200) in the contralateral non-ischemic (gray bar) and ischemic (black bar) limbs. Results are shown as the mean ± S.E. (n = 5/group). ANOVA with post-hoc Tukey HSD. **i**, LysM-Wnt5a^{GOF} mice received intra-peritoneal anti-VEGF-A$_{165}$b neutralizing monoclonal antibody (100 μg) on 0, 3 and 7 days after surgery. Non-specific mouse IgG was administered in a similar manner to control mice. Quantitative analysis of the ischemic/non-ischemic laser Doppler blood flow ratio in LysM-Wnt5a^{GOF} mice treated with control IgG or anti-VEGF-A$_{165}$b neutralizing antibody through postoperative day 28. Results are shown as the mean ± S.E. (n = 10/group). Repeated measures ANOVA. Quantitative analysis of capillary density by anti-CD31 antibody staining in LysM-Wnt5a^{GOF} mice receiving control IgG or anti-VEGF-A$_{165}$b on postoperative day 28. Capillary density was expressed as the number of capillaries per high power field (×200) in the contralateral non-ischemic (gray bar) and ischemic (black bar) limbs. Results are shown as the mean ± S.E. (n = 5/group). ANOVA with post-hoc Tukey HSD. *P < 0.05, **P < 0.01, ***P < 0.001.

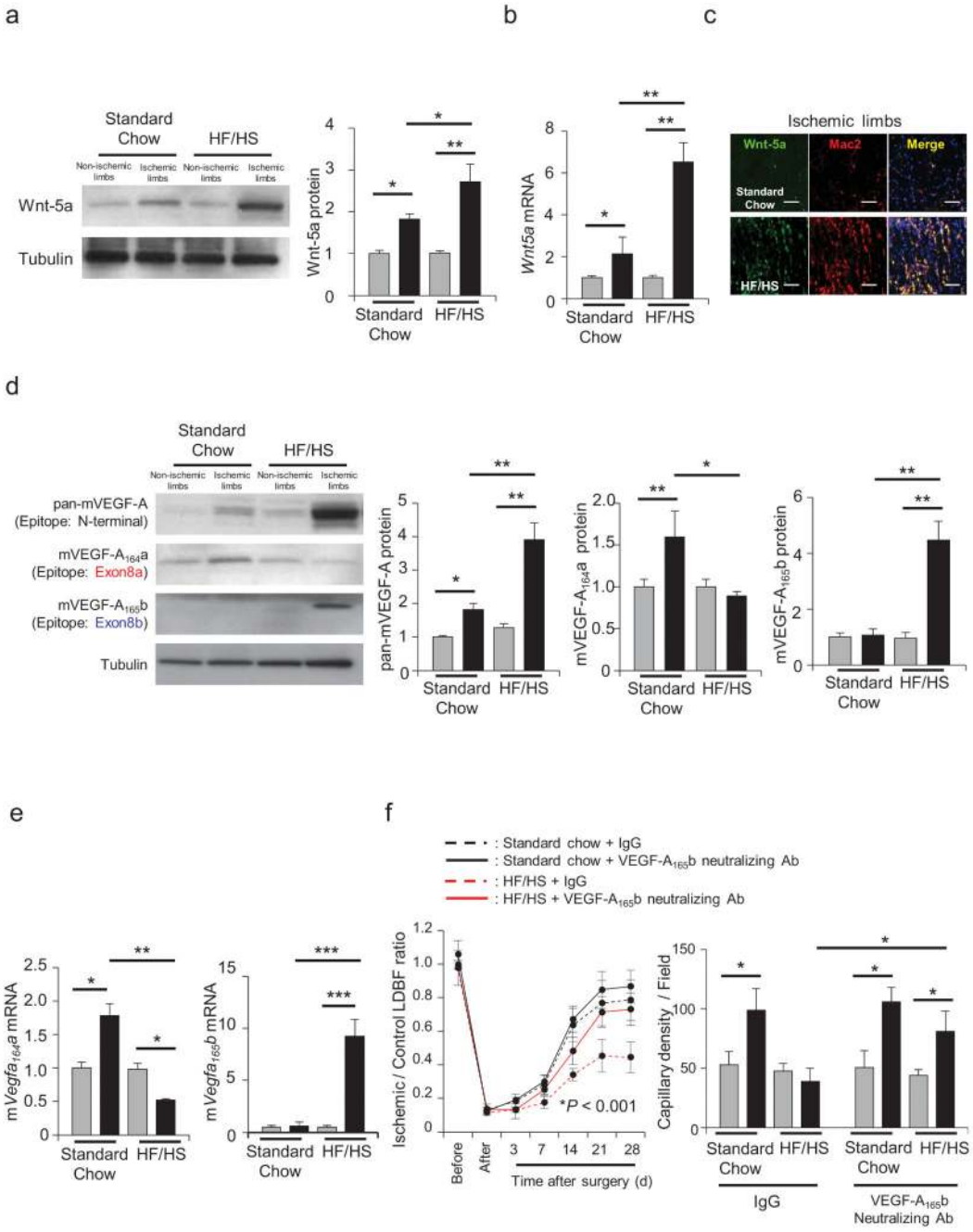

Figure 3. VEGF-A$_{165}$b impairs ischemia-induced angiogenesis in diet-induced obese mice

a, Wnt-5a protein levels were determined by western blot analysis in the contralateral non-ischemic (gray bar) and ischemic (black bar) muscle at 3 days after surgery. A representative blot from three independent experiments is shown. Relative Wnt-5a protein level was quantified using ImageJ. Immunoblots were normalized to tubulin signal. Results are shown as the mean ± S.E. (n = 5/group). ANOVA with post-hoc Tukey HSD. **b**, *Wnt5a* mRNA expression was measured by qRT-PCR in contralateral non-ischemic (gray bar) and ischemic (black bar) muscle at 3 days after surgery. Results are shown as the mean ± S.E. (n

Europe PMC Funders Author Manuscripts

= 5/group). ANOVA with post-hoc Tukey HSD. **c**, Top or Bottom: representative pictures of immunostaining for Wnt-5a and Mac2 in the ischemic limbs from mice fed standard chow or high fat/high sucrose diet. Scale bars are 100 μm. **d**, Total mVEGF-A, mVEGF-A_{164}a and mVEGF-A_{165}b protein levels were determined by western blot analysis in contralateral non-ischemic (gray bar) and ischemic (black bar) muscle at 7 days after surgery. A representative blot from three independent experiments is shown. Relative levels of pan-mVEGF-A, mVEGF-A_{164}a and mVEGF-A_{165}b protein were normalized to tubulin signal and quantified using ImageJ. Results are shown as the mean ± S.E. (n = 5/group). ANOVA with post-hoc Tukey HSD. **e**, Levels of m*Vegfa*$_{164}$*a* and m*Vegfa*$_{165}$*b* mRNA expression were measured by qRT-PCR in the non-ischemic (gray bar) and ischemic (black bar) muscle at 7 days after surgery. Results are shown as the mean ± S.E (n = 5/group). ANOVA with post-hoc Tukey HSD. **f**, Diet-induced obese mice received intraperitoneal anti-VEGF-A_{165}b neutralizing monoclonal antibody or non-specific mouse IgG (100 μg) on 0, 3 and 7 days after surgery. Quantitative analysis of the ischemic/non-ischemic laser Doppler blood flow ratio in diet-induced obese mice treated with control IgG or anti-VEGF-A_{165}b neutralizing antibody was observed through postoperative day 28. Results are shown as the mean ± S.E. (n = 10/group). Repeated measures ANOVA. Post-hoc Tukey HSD HF/HS + IgG vs. HF/HS + anti-VEGF-A_{165}b neutralizing antibody $P = 0.01$, vs. Standard Chow + IgG $P < 0.001$. Quantitative analysis of capillary density in diet-induced obese mice treated with control IgG or anti-VEGF-A_{165}b neutralizing antibody on postoperative day 28. Capillary density was expressed as the number of capillaries per high power field (×200) contralateral non-ischemic (gray bar) and ischemic (black bar) muscle. Results are shown as the mean ± S.E. (n = 5/group). ANOVA post-hoc Tukey HSD. *$P < 0.05$, **$P < 0.01$, ***$P < 0.001$.

Europe PMC Funders Author Manuscripts

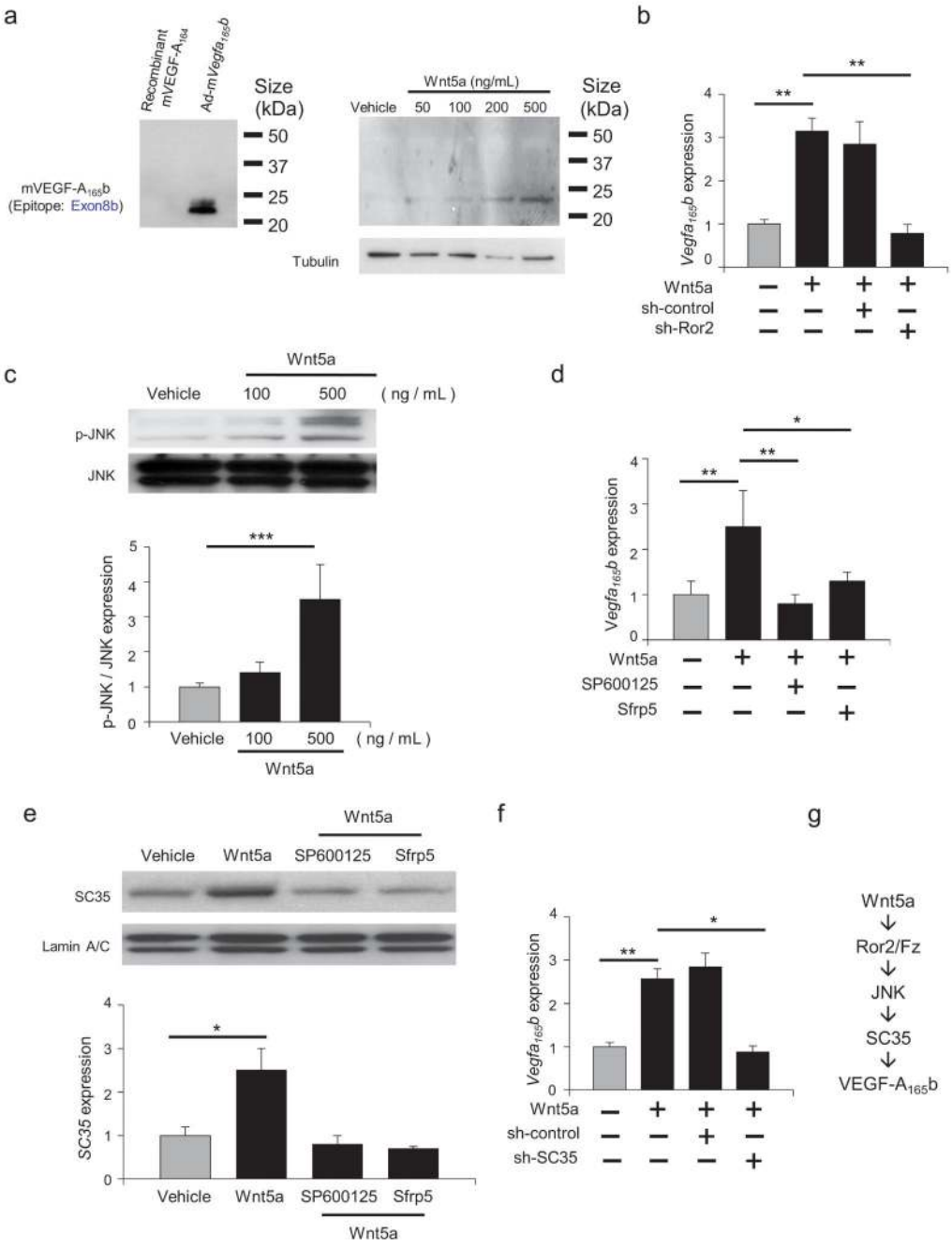

Figure 4. Wnt5a regulate VEGF-A_{165}b expression via Ror2/JNK/SC35-dependent mechanism in macrophages

a. VEGF-A_{165}b protein expression was measured by western immunoblot analysis in the presence or absence of recombinant Wnt5a in cultured RAW264.7 cells after treatment for 24 hours. **b.** *$Vegfa_{165}b$* mRNA expression was measured by qRT-PCR 8 hours after treatment with Wnt5a (500 μg/ml) or vehicle in RAW264.7 cells that had been pre-incubated with vehicle, sh-control or sh-Ror2. ANOVA with post-hoc Tukey HSD. **c.** Phosphorylation of JNK (p-JNK) was measured by western blot analysis in cells treated with

Europe PMC Funders Author Manuscripts

or without recombinant Wnt5a for 30 minutes. Relative phosphorylation levels of JNK were quantified by using ImageJ. Results are shown as the mean ± S.E. (n = 3/group). ANOVA with post-hoc Tukey HSD. **d.** The effects of JNK inhibition and Sfrp5 treatment or Wnt5a-induced *Vegfa*$_{165}$*b* expression. *Vegfa*$_{165}$*b* mRNA expression was measured by qRT-PCR. SP600125 was added 10 minutes prior to the addition of recombinant Wnt5a (500 ng/ml). Recombinant Sfrp5 was added at 1 μg/ml. Results are shown as the mean ± S.E. (n = 3/group). ANOVA with post-hoc Tukey HSD. **e.** SC35 protein expression was measured by western blot analysis in the presence or absence of stimulation with recombinant Wnt5a. The effects of the JNK inhibitor SP600125 or Sfrp5 on Wnt5a-induced SC35 expression were evaluated at 1 hour. Relative levels of SC35 were quantified by using ImageJ. Immunoblots were normalized to LaminA/C signal. Results are shown as the mean ± S.E. (n = 3/group). ANOVA with post-hoc Tukey HSD. **f.** SC35 is essential for *Vegfa*$_{165}$*b* expression. *Vegfa*$_{165}$*b* mRNA expression was measured by qRT-PCR. Cells were treated with sh-control and sh-SC35 for 8 hours and treated with or without recombinant Wnt5a. ANOVA with post-hoc Tukey HSD. **g.** Graphic scheme of proposed mechanism. *P < 0.05, **P < 0.01, ***P < 0.001.